



Published in final edited form as:

*Stem Cell Res.* 2021 May ; 53: 102354. doi:10.1016/j.scr.2021.102354.

## Generation of fourteen isogenic cell lines for Parkinson's disease-associated leucine-rich repeat kinase (LRRK2)

Aleksandra Beylina<sup>#1</sup>, Rebekah G. Langston<sup>#1</sup>, Dorien Rosen<sup>1</sup>, Xylena Reed<sup>1</sup>, Mark R. Cookson<sup>1,\*</sup>

<sup>1</sup>Laboratory of Neurogenetics, National Institute on Aging, National Institutes of Health, Bethesda, MD 20892, USA

# These authors contributed equally to this work.

### Abstract

Mutations in leucine-rich repeat kinase 2 (LRRK2) are associated with inherited forms of Parkinson's disease (PD), causing disease by a gain of kinase function. Here, we describe a series of isogenic iPSC lines with any of five pathogenic mutations (N1437H, R1441C, Y1699C, G2019S and I2020T); two hypothesis testing mutations (GTP binding null, T1348N, and kinase dead, K1906M) and two LRRK2 knockouts. This resource could be used to assess effects of mutations on the function of endogenous LRRK2 and/or to study LRRK2 interactors and substrates in iPSC-derived cellular models.

### 1. Resource Table

---

Unique stem cell lines identifier	NIAi001-A
	NIAi001-B
	NIAi001-C
	NIAi001-D
	NIAi001-E
	NIAi001-F
	NIAi001-G
	NIAi001-H
	NIAi001-I
	NIAi001-K
	NIAi001-L
	NIAi001-M
	NIAi001-N

---

This is an open access article under the CC BY-NC-ND license.

\*Corresponding author.

Declaration of Competing Interest

The authors declare that they have no known competing financial interests or personal relationships that could have appeared to influence the work reported in this paper.

Alternative names of stem cell lines	LRRK2 I2020T PL2F4 (NIAi001-A) LRRK2 I2020T PL2D7 (NIAi001-B) LRRK2 G2019S PL2A9 (NIAi001-C) LRRK2 G2019S PL2H7 (NIAi001-D) LRRK2 Y1699C PL3H2 (NIAi001-E) LRRK2 Y1699C PL2H7 (NIAi001-F) LRRK2 R1441C PL2F5 (NIAi001-G) LRRK2 R1441C PL3C2 (NIAi001-H) LRRK2 N1437H PL3D7 (NIAi001-I) LRRK2 N1437H PL3F5 (NIAi001-J) LRRK2 K1906M PL2H7 (NIAi001-K) LRRK2 T1348N PL1B6 (NIAi001-L) LRRK2 KO PL1C4 (NIAi001-M) LRRK2 KO PL1C6 (NIAi001-N)
Institution	National Institutes of Health, National Institute on Aging
Contact information of distributor	Mark Cookson: cookson@mail.nih.gov
Type of cell lines	iPSC
Origin	Human
Cell Source	A18945 (Thermo Scientific, cat # A18945)
Clonality	Clonal
Method of reprogramming	A18945 cell line was derived from CD34 + cord blood using a three-plasmid, seven-factor (SOKMNL; SOX2, OCT4 (POU5F1), KLF4, MYC, NANOG, LIN28, and SV40L T antigen) EBNA-based episomal system
Multiline rationale	Isogenic clones
Gene modification	Yes
Type of modification	Induced mutation
Associated disease	Parkinson's disease
Gene/locus	LRRK2/PARK8
Method of modification	CRISPR/Cas9
Name of transgene or resistance	N/A
Inducible/constitutive system	N/A
Date archived/stock date	N/A
Cell line repository/bank	N/A
Ethical approval	Original line obtained from Thermo Scientific. Ethical license/patient consent: -45 CFR Part 46, IRB SOP RR 404.

## 2. Resource utility

This unique set of lines will be an important resource for the PD community to study effects of LRRK2 mutations in cell lines expressing endogenous levels of LRRK2. Studies with models derived from these iPSC lines could help determine the roles of different cell types in PD pathogenesis.

### 3. Resource details

Leucine-rich repeat kinase 2 (LRRK2) encodes a large (2527 amino acid) multidomain protein with kinase and GTPase enzymatic domains. Mutations in LRRK2 are associated with autosomal dominant familial Parkinson's disease (Nalls et al., 2019; Paisan-Ruiz et al., 2004). Seven mutations in LRRK2 have been demonstrated to be pathogenic: N1437H, R1441C/G/H, Y1699C, G2019S and I2020T (Rudenko et al., 2012). Most data suggests that LRRK2 mutations induce a gain of function while loss of function variants are not associated with PD risk. Prior studies indicate that LRRK2 may play a role in lysosomal biology, vesicle trafficking, cytoskeletal maintenance, and the immune system, but how these relate to PD pathogenesis is uncertain (Cookson, 2015). Looking for common effects of mutations that are not shared with loss of function variants may help resolve this question.

We created five PD pathogenic mutations in heterozygous and homozygous states, as well as GTP-binding null (T1348N) and kinase dead (K1906M) mutations and two LRRK2 knockout lines (Table 1). We used CRISPR/Cas9 technology to introduce all of these mutations into a single female iPSC background, A18945 (TMOi001-A). CRISPR-Cas9 gRNAs within 10–15 bp of each mutagenesis site were selected based on low off-target risk and high on-target potential. LRRK2 knockout (KO) lines were made using two gRNAs targeting the T1348 and K1906 regions of LRRK2. Knock-in mutations were introduced by using donor oligos (DO) with the desired mutation. Additional variants were introduced into some donor oligos to disrupt the CRISPR-Cas9 binding site, and improve editing efficiency, without changing amino acid sequences. Three 96 well plates per mutation were picked and analyzed by Sanger sequencing. Positive clones were expanded and sequenced again to confirm mutations (Fig. 1C, Table 2). To verify clonal purity, and homozygosity, and heterozygosity of the introduced variants we submitted clones for targeted amplicon sequencing and performed Amplican analysis. Pluripotency of the verified iPSC lines was validated by expression of the pluripotency markers: OCT4, SOX2, and NANOG as shown by immunocytochemistry (Fig. 1A, Table 2). Quantitative assessment showed that more than 94% of cells were positive for markers essential for pluripotency, OCT3/4 and SSEA-4 in all iPSC lines (Fig. 1B, Table 2). OCT3/4 was assessed by ICC, and SSEA-4 by flow cytometry. All iPSC lines have a normal female karyotype (46, XX) without any obvious aberrations (Supplementary Fig. 1, Table 2). Short tandem repeat (STR) analysis of 16 genomic loci showed 100% identical polymorphisms in the parental iPSC line and all derived iPSC lines (archived at journal; available from authors). The differentiation potential of the iPSC lines was confirmed by targeted differentiation into cells of all three germ layers. Immunocytochemistry confirmed expression of SOX17 and  $\alpha$ -fetoprotein (AFP) (endoderm); alpha-muscle actin (<SMA) and Brachyury (mesoderm); and Nestin and MAP2 (ectoderm) (Fig. 1D, Table 2). All generated iPSC lines were free of mycoplasma contamination (Supplementary Fig. 1B, Table 2). In conclusion, we generated knockin and knockout iPSC lines to support studies of LRRK2-related neurodegeneration in human cellular models.

## 4. Materials and methods

### 4.1. Growth, propagation and morphology of iPSC lines.

A18945 cell line and isogenic clones derived from this line were grown in E8 media (Thermo Scientific, cat #A1517001). 10 $\mu$ M Rock inhibitor (STEMCELL, Cat # 72304) was added to E8 media for 18–24 h after splitting and thawing. iPSC clones were frozen in Synth-A-Freeze Cryopreservation media (Thermo Scientific, Cat # A1254201).

### 4.2. Genome editing of A18945 iPSC line using RNPs

**4.2.1. RNP complex formation**—Alt-R CRISPR-Cas9 guide RNA (crRNA) were custom designed using the IDT website [https://www.idtdna.com/site/order/designtool/index/CRISPR\\_CUSTOM](https://www.idtdna.com/site/order/designtool/index/CRISPR_CUSTOM) based on low off-target risk and high on-target potential. Alt-R CRISPR-Cas9 crRNAs for each targeted region are shown in Table 3. Alt-R CRISPR-Cas9 crRNA and Alt-R CRISPR-Cas9 tracrRNA (IDT, cat # 1072533) were resuspended in nuclease-free duplex buffer (IDT, cat# 11010301) to 200  $\mu$ M. Five  $\mu$ l of 200  $\mu$ M crRNA and 5  $\mu$ l of 200  $\mu$ M tracrRNA were mixed together and heated at 95°C for 5 min and then the mixture was cooled to RT. Next, 1.7  $\mu$ l (104 pmol) of Alt-R S.p. Cas9 nuclease (IDT, cat # 1081058) were mixed together with 1.2  $\mu$ l (120 pmol) Alt-R CRISPR-Cas9 crRNA/tracrRNA duplex and 2.1  $\mu$ l of 1xPBS solution and incubated 30 min at RT.

**4.2.2. ssDO preparation**—Single stranded donor oligos (ssDO) with the desired mutations (see Table 3) were synthesized by IDT and resuspended in DPBS at a concentration of 100 pmol/ $\mu$ l.

**4.2.3. Nucleofection**—70–80% confluent iPSC were dissociated into single cells using Accutase (Thermo Scientific, cat # A1110501) and counted using a TC20 Automated Cell Counter (Bio-Rad). iPS cells ( $8 \times 10^5$  per sample) were pelleted at 1000 rpm for 3 min and cell pellet were gently resuspended in 100  $\mu$ l of P3 Primary Cell Solution (Lonza, PBP3–02250). Immediately prior to nucleofection, 2  $\mu$ l (100 pmol/ $\mu$ l) of ssDO was added to 5  $\mu$ l of pre-assembled Cas9/RNP. One hundred  $\mu$ l of iPS cells resuspended in P3 primary cell solution were transferred to the tube containing Cas9/RNP complexes and ssDO. Cells were mixed twice with Cas9/RNP/Donor oligo and the mixture was transferred to the 100  $\mu$ l nucleocuvette (Lonza; 2022–01). iPSC were nucleofected immediately using the ‘Primary Cell P3’ program and ‘CA-137’ pulse code. After nucleofection, iPSC were transferred using a Lonza disposable Pasteur pipette into one well of a Matrigel-coated 6-well plate containing 3 mL E8 media with 10  $\mu$ M Rock inhibitors. Cells were cultured in a 32°C/5% CO<sub>2</sub> incubator for two days and then transferred to a 37°C incubator. Edited iPSC pools were expanded, frozen, and used for generation of clones from single cells.

### 4.3. Generation of clones from single cell

Expanded pools were dissociated with Accutase, counted, and 10,000 single cells were plated on 10 cm Matrigel-coated dishes containing E8 media with 10  $\mu$ M Rock inhibitor for two days. Subsequently, the media was changed without Rock for 5–7 days. Single cell colonies were expanded to 250–500  $\mu$ M diameter and picked using a 100  $\mu$ l pipet tip under a Bioimager microscope. Individual colonies were transferred to Matrigel-coated 96-well

plates. Three 96 well plates per mutation were picked and expanded until 70–80% confluency. Each expanded plate was split into two plates: half of the cells were transferred onto a new 96 well plate for further propagation and half of the cells were used for sequencing analysis.

#### 4.4. Sequencing

Plates with collected cells were centrifuged at 3,000 rpm for 5 min and resuspended in 30  $\mu$ l of water. Cells were heated at 95° C for 10 min and 2  $\mu$ l of cells were used for PCR with region specific primers listed in Table 3. PCR was carried out using Terra polymerase (Takara Bio). Each PCR product was sequenced using forward and reverse primers with Applied Biosystems BigDye terminator v3.1 sequencing chemistry according to manufacturer's instructions. The products were cleaned using Agencourt CleanSEQ reagent (Beckman Coulter), run on a 3730xl DNA analyzer (Applied Biosystems, Hitachi) and analyzed with Sequencher software. Positive clones were expanded and re-sequenced.

#### 4.5. Amplicon sequencing

Amplicon sequencing of pools and individual clones was performed by Psomagen using MiSeq Nano (250PE) sequencing on Illumina platform. Amplicon sequencing primers are listed in Table 3. FASTQ files for each sample were analyzed using the ampliCan tool in R (Labun et al., 2019).

#### 4.6. Karyotyping and STR analysis

Karyotyping and STR analysis were performed by WiCell Research Institute.

#### 4.7. Mycoplasma detection

Mycoplasma test was performed using PCR (ATCC, cat # 30–1012K). Positive control PCR was performed for the LRRK2 gene with the primers listed in Table 3.

#### 4.8. Pluripotency assessment

iPSC clones were grown on Matrigel-coated coverslips, fixed with 4% PFA, and stained with pluripotency markers listed in Table 3. Images were taken on a Zeiss 880 confocal microscope. The percentage of cells positive for OCT3/4 was calculated on immunofluorescence images using the Fiji software. SSEA4 quantifications were performed by flow cytometry using PE-SSEA4 antibody (Table 3). At least 5,000 cells per sample were acquired and analyzed using BD FACs Diva 8.01 analysis software.

#### 4.9. Differentiation potential

iPSC clones were differentiated into three layers according to STEMdiff™ Trilineage Differentiation Kit (StemCell, Cat# 05230), fixed in 4% PFA, and stained with differentiation markers listed in Table 3. Images were taken on a Zeiss 880 confocal microscope.

## Supplementary Material

Refer to Web version on PubMed Central for supplementary material.

## Acknowledgement

This research was supported entirely by the Intramural research Program of the NIH, National institute on Aging.

## References

- Cookson MR, 2015. LRRK2 pathways leading to neurodegeneration. *Curr. Neurol. Neurosci. Rep* 15 (7), 42. Epub 2015/05/27. doi: 10.1007/s11910-015-0564-y. [PubMed: 26008812]
- Labun K, Guo X, Chavez A, Church G, Gagnon JA, Valen E, 2019. Accurate analysis of genuine CRISPR editing events with ampliCan. *Genome Res* 29 (5), 843–847. Epub 2019/03/10. doi: 10.1101/gr.244293.118. [PubMed: 30850374]
- Nalls MA, Blauwendraat C, Vallerga CL, Heilbron K, Bandres-Ciga S, Chang D, et al., 2019. Identification of novel risk loci, causal insights, and heritable risk for Parkinson's disease: a meta-analysis of genome-wide association studies. *Lancet Neurol* 18 (12), 1091–1102. Epub 2019/11/09. doi: 10.1016/S1474-4422(19)30320-5. [PubMed: 31701892]
- Paisan-Ruiz C, Jain S, Evans EW, Gilks WP, Simon J, van der Brug M, et al., 2004. Cloning of the gene containing mutations that cause PARK8-linked Parkinson's disease. *Neuron* 44 (4), 595–600. Epub 2004/11/16. doi: 10.1016/j.neuron.2004.10.023. [PubMed: 15541308]
- Rudenko IN, Chia R, Cookson MR, 2012. Is inhibition of kinase activity the only therapeutic strategy for LRRK2-associated Parkinson's disease? *BMC Med* 10, 20. Epub 2012/03/01. doi: 10.1186/1741-7015-10-20. [PubMed: 22361010]

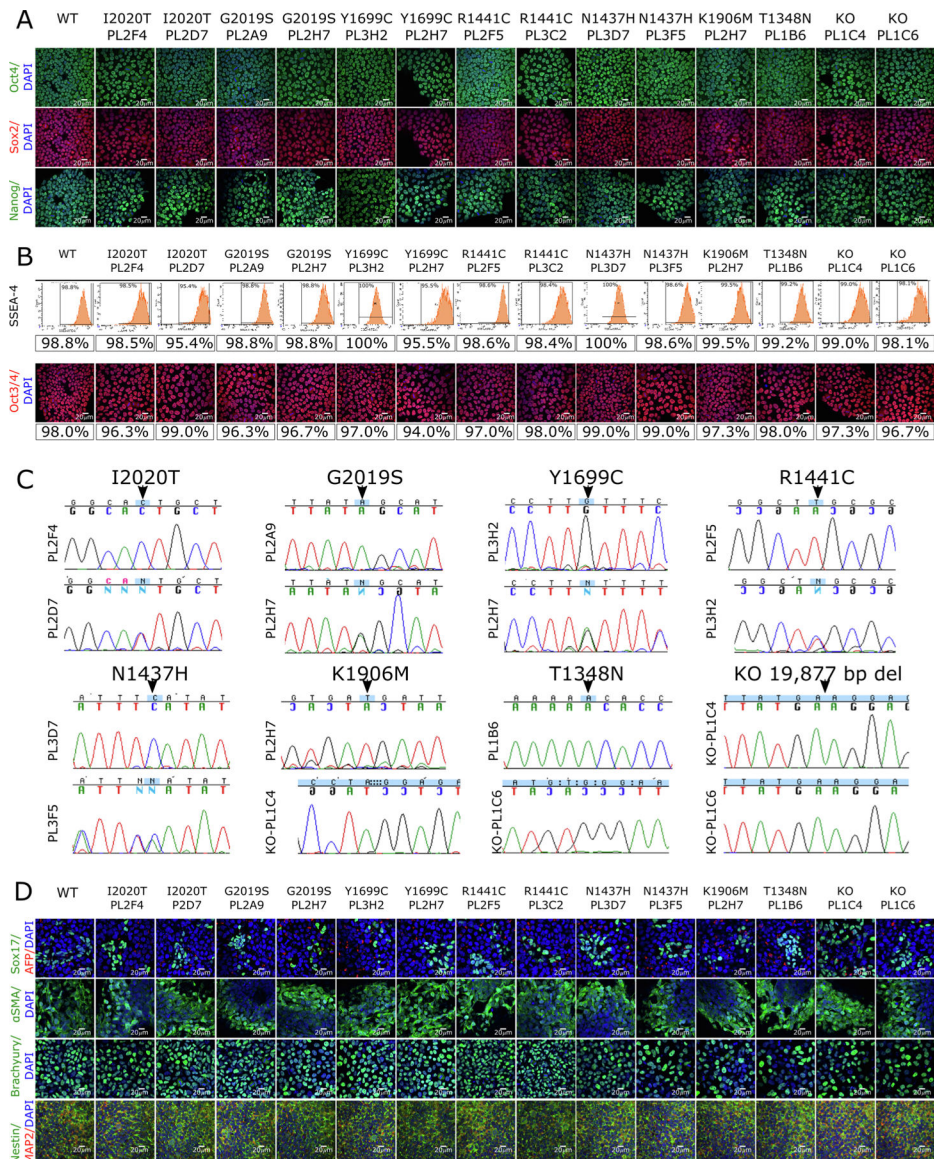


**Fig. 1.** Generation of lines with *LRRK2* mutations on an isogenic background. (A) iPSC lines carrying the indicated mutations (WT = wild type, KO = knockout; clone ID below each mutation) were stained for pluripotency markers OCT4 (top panels, green), SOX2 (middle panels, red) and NANOG (lower panels, green) and counterstained with the nuclear stain DAPI (blue, all panels). Scale bars = 20  $\mu$ m. (B) Quantitative analysis of SSEA-4 expression by flow cytometry (upper panels) or by staining for Oct3/4 (lower panels; red is Oct3/4, blue is DAPI; Scale bars = 20  $\mu$ m) allowed percentages of pluripotent cells to be estimated as indicated. (C) Sequence chromatograms of *LRRK2* coding changes, where upper panels show homozygous and lower panels show heterozygous clones. (D) Differentiation potential was assessed using immunostaining for endodermal markers SOX17 (green, first row) and  $\alpha$ -fetoprotein (AFP, red, first row); mesodermal markers alpha-muscle actin (SMA, green, second row) and Brachyury (green, third row); and ectodermal markers Nestin (green, fourth

row) and MAP2 (red, fourth row). All cells were counterstained with the nuclear dye DAPI (blue) and scale bars = 20  $\mu\text{m}$ .

Author Manuscript

Author Manuscript

Author Manuscript

Author Manuscript



Table 1

Summary of lines.

iPS line names	Abbreviation in figures	Gender	Age	Ethnicity	Genotype of locus	Disease
NIAi001-A	I2020T PL2F4	Female	Neonate	Unknown	I2020T homozygous mutation in LRRK2 gene	Parkinson disease
NIAi001-B	I2020T PL2D7	Female	Neonate	Unknown	I2020T heterozygous mutation in LRRK2 gene	Parkinson disease
NIAi001-C	G2019S PL2A9	Female	Neonate	Unknown	G2019S homozygous mutation in LRRK2 gene	Parkinson disease
NIAi001-D	G2019S PL2H7	Female	Neonate	Unknown	G2019S heterozygous mutation in LRRK2 gene	Parkinson disease
NIAi001-E	Y1699C PL3H2	Female	Neonate	Unknown	Y1699C homozygous mutation in LRRK2 gene	Parkinson disease
NIAi001-F	Y1699C PL2H7	Female	Neonate	Unknown	Y1699C heterozygous mutation in LRRK2 gene	Parkinson disease
NIAi001-G	R1441C PL2F5	Female	Neonate	Unknown	R1441C homozygous mutation in LRRK2 gene	Parkinson disease
NIAi001-H	R1441C PL3C2	Female	Neonate	Unknown	R1441C heterozygous mutation in LRRK2 gene	Parkinson disease
NIAi001-I	N1437H PL3D7	Female	Neonate	Unknown	N1437H homozygous mutation in LRRK2 gene	Parkinson disease
NIAi001-J	N1437H PL3F5	Female	Neonate	Unknown	N1437H heterozygous mutation in LRRK2 gene	Parkinson disease
NIAi001-K	K1906M PL2H7	Female	Neonate	Unknown	K1906M homozygous mutation in LRRK2 gene	Parkinson disease
NIAi001-L	T1348N PL1B6	Female	Neonate	Unknown	T1348N homozygous mutation in LRRK2 gene	NIAi001-K
NIAi001-M	LRRK2 KO PL1C4	Female	Neonate	Unknown	c.5694_5697delTTGAA (p.Ile1339LysfsX12)	NIAi001-L
NIAi001-N	LRRK2 KO PL1C6	Female	Neonate	Unknown	c.4015_4018delATTG (p.Ile1339TrpfsX15) and c.4016_4985del (p.Ile1339LysfsX12) mutations in LRRK2 gene	NIAi001-M

Table 2

## Characterization and validation.

Classification	Test	Result	Data
Morphology	Photography	All iPSC lines are morphologically normal	Not shown; available from authors
Phenotype	Qualitative analysis	Confirmed expression of pluripotency markers: OCT4, NANOG, and SOX2	Fig. 1 panel A
	Quantitative analysis	Assessed % of positive cells for pluripotency marker, OCT3/4 by immunocytochemistry counting and cell surface markers, SSEA-4 by flow cytometry. All lines are more than 94% positive for both markers.	Fig. 1 panel B
Genotype	Karyotype (G-banding) and resolution	1. 46XX, Resolution 425–500	Supplementary panel A
		2. 46XX, Resolution 350–450	
		3. 46XX, Resolution 400–500	
		4. 46XX, Resolution 400–450	
		5. 46XX, Resolution 425–550	
		6. 46XX, Resolution 425–475	
		7. 46XX, Resolution 425–500	
		8. 46XX, Resolution 400–425	
		9. 46XX, Resolution 475–550	
		10. 46XX, Resolution 425–500	
		11. 46XX, Resolution 475–550	
		12. 46XX, Resolution 375–450	
		13. 46XX, Resolution 425–500	
		14. 46XX, Resolution 450–475	
		15. 46XX, Resolution 400–525	
Identity	Microsatellite PCR (mPCR) OR STR analysis	STR analysis 16 specific loci were tested. All isogenic lines matched 100%.	Supplementary data 1 Submitted in archive with journal
	Sequencing		Fig. 1 panel C
Mutation analysis (IF APPLICABLE)	Sequencing	1. I2020T PL2F4-homozygous	
		2. I2020T PL2D7-heterozygous	
		3. G2019S PL2A9-homozygous	
		4. G2019S PL2H7-heterozygous	
		5. Y1699C PL3H2-homozygous	
		6. Y1699C PL2F7-heterozygous	
		7. R1441C PL2F5-homozygous	

Appendix A. Supplementary data

Supplementary data to this article can be found online at <https://doi.org/10.1016/j.scr.2021.102354>.

Classification	Test	Result	Data
			8. R1441C PL3C2-heterozygous
			9. N1437H PL3D7-homozygous
			10. N1437H PL3F5-heterozygous
			11. K1906M PL2H7-homozygous
			12. T1348N PL1B6-homozygous
			13. KO PL1C4-c.5694_5697delTGAA (p.Tyr1898Ter) and c.4016_4985del (p.Ile1339LysfsX12)
			14. KO PL1C6-c.4015_4018delATTG (p.Ile1339TrpfsX15) and c.4016_4985del (p.Ile1339LysfsX12)
	Southern Blot OR WGS	Not performed	N/A
Microbiology and virology	Mycoplasma	Mycoplasma testing was done by RT-PCR. All clones-negative	Supplementary Fig. 1
Differentiation potential	e.g. Embryoid body formation OR Teratoma formation OR Scorecard OR Directed differentiation	The STEMdiff™ Trilineage Differentiation Kit (StemCell) was used to test differentiation potential. We confirmed the expression of endoderm (AFP, SOX-17), mesoderm (<-SMA, Brachyury) and ectoderm (Nestin, MAP2) markers in all clones.	Fig. 1 panel D
Donor screening (OPTIONAL)	HIV 1 + 2 Hepatitis B, Hepatitis C	Not performed	N/A
Genotype additional info (OPTIONAL)	Blood group genotyping	Not performed	N/A
	HLA tissue typing	Not performed	N/A

Author Manuscript

Author Manuscript

Author Manuscript

Author Manuscript

Company Cat # and RRID	
Millipore, Cat# MAB4423, RRID:AB_11213224	
BioLegend Cat# 330406, RRID:AB_1089206	
Santa Cruz Biotechnology Cat# sc5279, RRID: AB_628051	
Abcam Cat #ab19557, RRID:N/A	
Millipore Cat# MABD24, RRID:AB_11203826	
Millipore Cat# ABD69, RRID:AB_2744681	
Santa Cruz Biotechnology Cat# sc-74422, RRID:AB_1126216	
Millipore Cat# 2004189, RRID: N/A	
R and D Systems Cat# AF1924, RRID:AB_355060	
R and D Systems Cat# AF2085, RRID:AB_2200235	
Novus Cat# NB300-978, RRID:AB_2273628	
Thermo Fisher Scientific Cat# A-21202, RRID:AB_141607	
Thermo Fisher Scientific Cat# A10037, RRID:AB_2534013	
Thermo Fisher Scientific Cat# A-21206, RRID:AB_2535792	
Thermo Fisher Scientific Cat# A-11055, RRID:AB_2534102	
Thermo Fisher Scientific Cat# A-11057, RRID:AB_2534104	

Author Manuscript

Author Manuscript

Author Manuscript

Author Manuscript

Company Cat # and RRID

TCACACTGTATCCCCTGGCTGCCATCATTTGCCAAAGATTGCTGATTATAGCATTGCTCAGTACTGTCTGTAGAAATGGGGATAAAACATCAGAGGGGCACACCAGGTAGGTGATCAGGTCTGTCTCATPAATTTCTATCTTCAGGATGGA  
 TCACACTGTATCCCCTGGCTGCCATCATTTGCCAAAGATTGCTGATTATAGCATTGCTCAGTACTGTCTGTAGAAATGGGGATAAAACATCAGAGGGGCACACCAGGTAGGTGATCAGGTCTGTCTCATPAATTTCTATCTTCAGGATGGA  
 CCATTGTGAGAACTCTGAAATTATCATTCGACTATATGAAAATGCCCTTGTTCCTCAATGGGATTTGGTCAAGATTAATCATCGATTACTTGAGATTTTCACCTTACATGCTTTCAGGGAGAGGTAAGTATCTAATGAAAGACT  
 AGGTTTGAAAAGGCAAAAGCAAGAGGGGTTTTTGGTCTCCAGGCTTGGCCCTCATCTCCCTGCTGATTCGTTGGCACACATTTAGATGTTTCTGATGAGAAAGCAACCGCAAGCCCTGCATCAGTAAATAATCACCAGGAACTC  
 GCTGTCTATGACCTCAAGCAAGGGCAAGGGCATGAAAGCCTTGGCTA TTTCAATAAAAGGTGATTTGTTCTGTATCATTTGAAAA TAGAAAAATAATTCATGTGCTGTGTGGCTGTGTGTGT GTGTGTGTAAAGTTA  
 CTTTTTCAAAAAGGTGATGGCAGTTTTGGATCAGTTTTACCGAGCTGCAGAGGAGAAAGTGGCTGTGATGATTTTTTAATAAACATACATCAGGCTGTAAAGACAAGTAAGAAAATTCATAATAATAATTAATAAAT  
 TTTATAACCGAATGAACTTATGATCGTGGGAAATACTGGGAGTGGTAAAAACACCTTATTGCACAATTAATGAAAACCAAGAAATCAGATCTTGGAAATGCAAAGTGCCACAGTTGGCATAGATGTGAAAAGACTGGCCATACC